Low frequency coherent modes in TJ-II Plasmas

B. J. Sun, D. López-Bruna, M. A. Ochando, M. A. Pedrosa

Laboratorio Naciónal de Fusion, Asociación EURATOM-CIEMAT, 28040-Madrid, Spain

Introduction

Two types of low frequency (<100 kHz) coherent modes are commonly seen in NBI plasmas [1, 2, 3, 4] of the TJ-II Heliac-type stellarator. One is fixed in the $E \times B$ frame (1st type), the other one (2nd type) moves in that frame with speeds within the electron diamagnetic drift range (i.e., within speeds $E \times B + u_{e*}$ in the laboratory frame). Only the 1st type survives in H-mode, but both types show electromagnetic fluctuations and related plasma transport, which is quite similar to quasi-coherent fluctuations in Alcator C-Mod [5], edge harmonic oscillation (EHO) in DIII-D [6] and ASDEX Upgrade [7]. These modes and their behavior in relation with the L-H transition might provide clear-cut arguments about the physical ingredients governing the transition process in TJ-II plasmas and, possibly, more general toroidal devices.

General phenomenology

Low frequency coherent modes appear in NBI plasmas of different magnetic configurations and plasma parameters when low order rational surfaces are located near the edge. By way of example, figures 1–4 correspond to a magnetic configuration with $\iota = 8/5$ located around normalized minor radius $\rho = 0.85$. ECH is used to start and heat the plasma, then co-NBI is turned on for further heating and fueling. The average density increases from 0.6 to 4.0 in 10^{19} m^{-3} units.

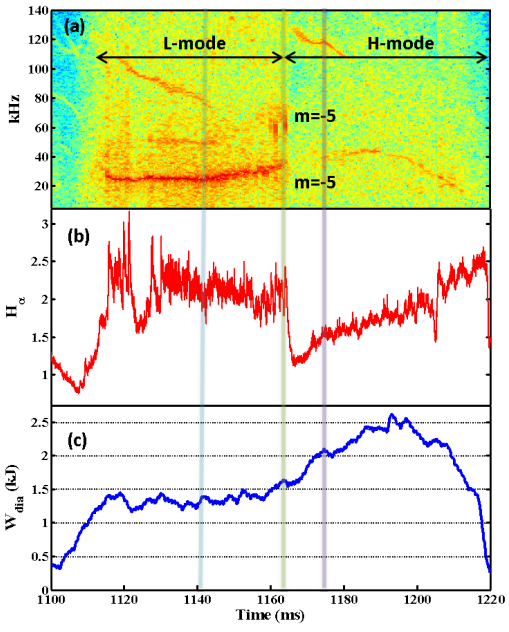

Figure 1: *Discharge #18998. (a) Mirnov signal spectrum, (b) H_α signal, (c) diamagnetic energy.*

In discharge #18998 (fig. 1(a)), a 1st type coherent mode with poloidal number $m = -5$ appears in the Mirnov coils when the plasma reheats after the ECH turn-off, around $t = 1115$ ms. At t=1142 ms, there is a slight H_α signal drop and the frequency starts to increase from 25 kHz to 37 kHz until an L-H transition appears at $t = 1164$ ms (fig. 1(b)), which causes a 20% increment in diamagnetic energy (fig. 1(c)). Just before the L-H transition, the 2nd type

mode appears and chirps down from 80 kHz to 50 kHz accompanied by a pulsing H_α signal.

At the L-H transition both modes are suppressed or strongly weakened. Then the diamagnetic energy increases rapidly in about 10 ms and the 1st type mode comes back with reduced amplitude despite the higher frequency ≈ 40 kHz. The frequency continues to increase to a maximum value around 45 kHz until it drops to 17 kHz. Note that during this H-mode phase the diamagnetic energy also first increases and then drops as a consequence of the plasma cooling due to electron energy unbalance. The 2nd type mode does not show up during the L-H transition and H mode. Aside from the magnetic fluctuations seen by Mirnov probes, the modes show electric perturbations as detected with Langmuir probes, which proves their electromagnetic nature. Associated particle transport is clearly seen in the corresponding $\langle \tilde{n} v_r \rangle$ flux spectrum shown in figure 2.

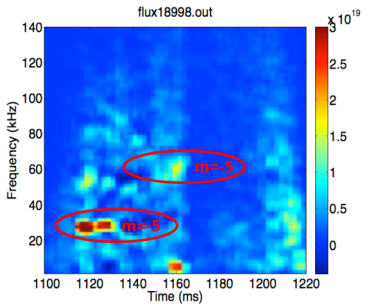

Figure 2: *Discharge # 18998. Flux spectrum from Langmuir probes.*

Figure 3 corresponds to a very similar discharge except that at $t = 1164$ ms, instead of directly undergoing an L-H transition, the plasma stays in L-mode with a prominent 2nd type mode. It is characterized by a higher frequency than type 1 and it most often chirps down, as in the example of fig. 3(a). Note the large pulsing in H_α light (fig. 3(b)) and the transport centered at the corresponding frequency in the $\langle \tilde{n} v_r \rangle$ flux spectrum, fig. 4. When present, this 2nd type mode precedes the L-H transition and seems to be related with the threshold conditions.

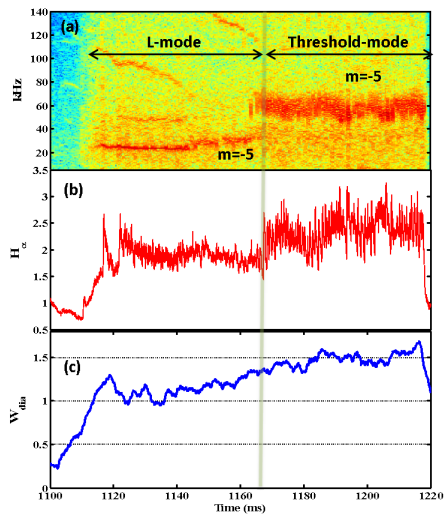

Figure 3: *Discharge #18997. (a) Mirnov signal spectrum, (b) H_α signal, (c) diamagnetic energy.*

This mode is associated with significant particle transport (see H_α activity in figure 3(b)) and prevents the transport barrier build up. Sometimes, depending on plasma parameters, type-1 mode can also play this role and show repetitive transport barrier breaking and H_α bursts.

Islands rotation

In a systematic survey of different magnetic configurations, both types of mode have been found to propagate in the electron diamagnetic drift direction originating frequencies that are proportional to the poloidal mode numbers of main near-edge magnetic resonances. Note that,

in high density and low temperature NBI plasmas, electron diamagnetic and ExB rotation share the same sign.

The frequency of the 1st type mode always starts from a non-zero value (which sets a lower limit), keeps rather constant during the L-mode phase slightly augmenting as the plasma approaches the L-H transition, and reaches its highest frequencies during the H-mode phase. During the L-mode phase at TJ-II the edge plasma is almost in rigid rotation, at least in co-NBI plasmas like the examples shown in figures 1 and 3. With the resonant $\iota = n/m$ placed around $\rho = 0.8$, the frequency per mode number f/m is always in the range 4.8–7.2 kHz. This is consistent with $f_{E\times B} = V_{E\times B}/2\pi a\rho$ = 6–7.5 kHz close to L-H transition and $f_{E\times B}$ = 4-6 kHz far from L-H transition [8] (a is the average minor radius). Likewise in H-mode case, the maximum f/m around 48 kHz/5 = 9.6 kHz agrees with $f_{E\times B}$ = 10–12.5 kHz at around $\rho = 0.8$ [8]. Figure 5 illustrates these facts for discharges where magnetic resonances of different m are placed around the $\rho = 0.8$ region. The linear fit gives the frequency per mode number.

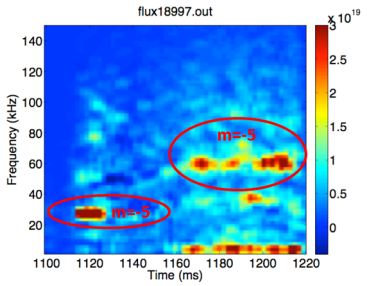

Figure 4: *Discharge # 18997. Flux spectrum from Langmuir probes.*

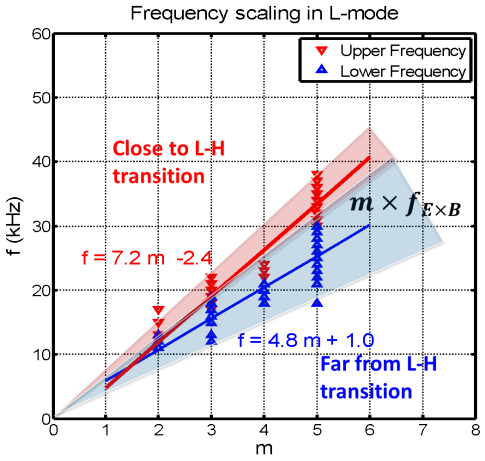

Figure 5: First type mode frequency scaling in L-Mode plasma

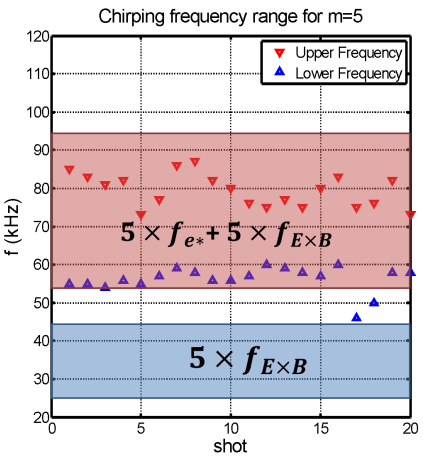

Figure 6: Second type mode chirp frequency range for m=5

The 2nd type mode always has a higher frequency than the 1st type and typically chirps down within a frequency range. Figure 6 is a plot of the upper (red triangles) and lower (blue triangles) frequencies found in 20 discharges from configurations where the dominant resonance corresponds to $m = 5$. The discharges correspond to different densities and NBI heating. The corresponding $f_{E\times B}$ in the $0.7 < \rho < 0.9$ region is marked with the blue band, while the red band

shows the frequencies obtained when the electron diamagnetic frequency for the corresponding plasma profiles is added. In more explicit terms, in co-NBI heated plasma with the rational surface around $\rho = 0.65$–0.75, the mode covers typical values $f/m = 9$–15 kHz, consistent with the electron diamagnetic rotation range in the $E \times B$ frame ($f_{e*} = V_{e*}/2\pi a\rho$ = 6–9 kHz, $f_{E\times B}$ = 7–9 kHz). In co+counter NBI plasmas with the rational surface around $\rho = 0.7$–0.8, $f/m = 11$–17 kHz also indicating $f_{e*} + f_{E\times B}$ range (f_{e*} = 6–9 kHz, $f_{E\times B}$ = 5–8 kHz).

Discussion

A survey of TJ-II plasmas sustained by NBI heating alone (densities around 2–5 10^{19} m^{-3}, core temperatures $T_e \sim 0.3$ keV and $T_i \sim T_e/2$) indicates that low frequency coherent modes (< 100 kHz) are due to the rotation of magnetic islands. Two types of mode are found. In the 1st type, rotation seems due to ExB motion alone, while a 2nd type appears to have a diamagnetic contribution. The results here presented suggest that some tearing mode dynamics originated in the local (i.e., in the resonant region) plasma profiles make the islands rotate either close to the ExB velocity or, after some bifurcation process, close to the ExB plus diamagnetic speeds. This could happen if the bifurcation consists of a disappearance of profile flattening in the resonant region [9]. The intimate link between these modes and the L-H transition process in these plasmas indicates that magnetic resonances play a fundamental role in the process, and the study of these low frequency modes may, therefore, give clear indications about the physics of L-H transitions.

Acknowledgement

This project has received funding from the European Union's Horizon 2020 research and innovation programme under grant agreement number 633053. The views and opinions expressed herein do not necessarily reflect those of the European Commission.

References

[1] I. García-Cortés et al Nucl. Fusion **40**, 1867 (2000)

[2] J A Jiménez et al Plasma Phys. Control. Fusion **48**, 515 (2006)

[3] B.Ph. van Milligen et al Nucl. Fusion **51**, 013005 (2011)

[4] B.Ph. van Milligen et al Nucl. Fusion **52**, 013006 (2012)

[5] Mazurenko, A., et al Phys. Rev. Lett. **89**, 225004 (2002)

[6] K H Burrell et al Plasma Phys. Control. Fusion **44**, A253 (2002)

[7] W Suttrop et al Plasma Phys. Control. Fusion **46**, A151 (2004)

[8] T Estrada et al Plasma Phys. Control. Fusion **51**, 124015 (2009)

[9] F. L. Waelbroeck, Nucl. Fusion **49** 104025 (2009)